future internet

MDPI

Article

Thermoelectric Generator-Powered Long-Range Wireless Real-Time Steam Leak Detection in Steam Traps

Raúl Aragonés [1,2], Joan Oliver [1] and Carles Ferrer [1,*]

[1] Department of Microelectronic and Electronic Systems, Universitat Autònoma de Barcelona, Bellaterra, 08193 Barcelona, Spain; raul.aragones@uab.cat (R.A.); joan.oliver@uab.cat (J.O.)
[2] R&D Department, AEInnova—Alternative Energy Innovations, S.L., AEInnova, 08224 Barcelona, Spain
* Correspondence: carles.ferrer@uab.cat

Abstract: This paper introduces a novel thermoelectric generator (TEG)-powered Industrial Internet of Things (IIoT) device that addresses key limitations in the detection of steam leaks in industrial steam pipelines, particularly in steam traps. Existing solutions often rely on battery-powered or wired sensors, which are limited by high maintenance costs, short lifespans, or significant infrastructure investments. The proposed device operates without batteries, using waste heat to provide continuous power, and leverages LoRaWAN for long-range wireless communication, minimizing reliance on costly internal infrastructure. Additionally, the device integrates temperature differential (ΔT) and ultrasonic sensors with edge computing capabilities to enhance real-time leak detection and reduce dependency on cloud computing. By enabling precise, low-maintenance monitoring of steam systems in energy-intensive industries (e.g., petrochemical, pharmaceutical), this technology can significantly reduce energy losses, operational costs, and greenhouse gas emissions. Initial testing demonstrates the device's ability to detect leaks accurately under varying industrial conditions, offering a robust, scalable solution for Industry 4.0 applications.

Keywords: steam trap; battery-less; TEG; LoRaWAN

Citation: Aragonés, R.; Oliver, J.; Ferrer, C. Thermoelectric Generator-Powered Long-Range Wireless Real-Time Steam Leak Detection in Steam Traps. *Future Internet* **2024**, *16*, 474. https://doi.org/10.3390/fi16120474

Academic Editors: Dionisis Kandris and Eleftherios Anastasiadis

Received: 10 October 2024
Revised: 10 December 2024
Accepted: 15 December 2024
Published: 19 December 2024

1. Introduction

The Internet of Things (IoT) is designed to connect physical objects to cloud computing infrastructure, enabling communication anytime and anywhere. In the industrial sector, this is referred to as the Industrial Internet of Things (IIoT), which plays a key role in the Industry 4.0 revolution. IIoT facilitates the real-time monitoring of machinery, leading to significant energy savings, reduced maintenance costs, fewer breakdowns, and decreased downtime. Consequently, the number of IoT devices deployed globally is expected to rise from the current 46 billion to 125 billion in the coming years [1]. However, despite the rapid increase in the number of these devices, the primary challenge for the future remains the energy supply for these systems [2].

Currently, most IIoT devices rely on lithium-based batteries, which present several environmental concerns, including the carbon footprint associated with their production, charging, and potential risks, particularly in hazardous environments where they may pose a fire or explosion hazard.

Regarding the environmental impact, Dirk Notz et al. [3] demonstrated a direct correlation between carbon emissions and Arctic ice melt. This study showed that Arctic ice has decreased by 50% over the past 40 years. At the UN Climate Conference in New York, new data further exacerbated these predictions. According to Professor Dirk Notz from the Max-Planck-Institute for Meteorology in Hamburg, Germany, every ton of CO_2 released into the atmosphere contributes to the melting of 3 square meters of Arctic ice [4]. This impact is illustrated in Figure 1, showing the Arctic ice melt per citizen according to data from *The Guardian* [5].

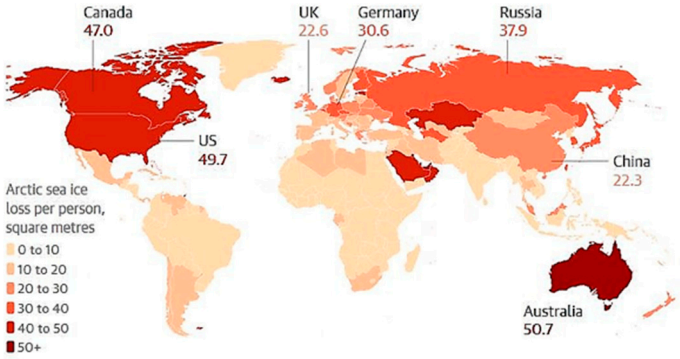

Figure 1. Arctic ice melting according to citizenship.

Energy-intensive industries, particularly those reliant on steam in their processes (such as oil and gas, chemical, petrochemical, pharmaceutical, and textile sectors), are among the largest contributors to greenhouse gas emissions. Over the past several years, these industries have increasingly acknowledged the impact of their emissions on climate change and have started improving their productivity, efficiency, and profitability through Industry 4.0 innovations. The deployment of IIoT technologies offers these industries the opportunity to further enhance their efficiency and become more environmentally sustainable. This includes sectors with explosive atmospheres (ATEX), such as the oil and gas, chemical, and petrochemical industries, which face unique challenges in implementing large-scale IoT sensing systems [6]. However, several difficulties remain in deploying IIoT devices in industrial environments, including the following:

- Energy requirements: Wired sensors require significant investment in infrastructure, with costs ranging between EUR 70 and 100 per meter of installation.
- Battery-powered wireless sensors: These devices involve high maintenance costs due to frequent battery replacement, averaging EUR 300 every 24 months.
- Short-range wireless protocols: To extend the battery life of IIoT devices, short-range protocols such as Bluetooth and WirelessHART are typically used. These protocols offer limited coverage, necessitating a substantial investment in wireless infrastructure, including routers and repeaters.
- Communications: Wired sensors also require significant investment in communication infrastructure, including cables, optical fiber channels, and switches.
- ATEX/EX environments: Wireless IIoT devices in these environments often use lithium batteries, with a risk of explosion, and thus cannot typically be deployed in oil and gas or petrochemical facilities.

In these industries with high energy demands, particularly those that use steam extensively in their processes, a major inefficiency relates to steam generation, transportation, and usage. For example, in a large oil refinery, steam circuits can span hundreds of kilometers, as steam is integral to various processes, including heating, cleaning, and power generation. Some refineries have up to 1000 km or more of piping dedicated to steam, chemicals, hydrocarbons, and water transportation. Steam traps are critical for the correct operation of these processes, where a mid-sized refinery contains between 10,000 and 20,000 steam traps.

The primary objective of this paper is to introduce a novel pre-commercial IIoT technology designed to detect steam leaks in steam traps. This device is powered by thermoelectric generators (TEGs), is maintenance-free, utilizes long-range wireless communication via LoRaWAN, and features edge computing for data preprocessing.

This paper is structured as follows: the next section introduces steam traps and their associated failures due to steam leaks, quantifying the economic impact of their failure. Section 3 discusses current detection methods, while Section 4 introduces the technological approach used in this project to detect steam leaks through temperature delta

(ΔT) detection and ultrasound sensors. Section 5 presents the results of a device installation in a pharmaceutical facility, and Section 6 concludes the paper with key findings.

2. Steam Trap Study

2.1. Steam Processes

Steam is widely used in major manufacturing industries such as the oil and gas, chemical, and petrochemical sectors due to its versatility and efficiency. It serves as a highly effective heat source for heating reactors and distillation columns, while also powering turbines to generate electricity for pumps and compressors. Steam is essential in refining processes like distillation and thermal cracking, as well as for cleaning and purifying equipment. Additionally, it provides a safer alternative to direct combustion heating, reducing risks of fire and explosions. In oil extraction, steam injection helps lower the viscosity of heavy oil, improving its extraction and transport. In summary, steam plays a critical role in transferring energy, driving machinery, enabling refining processes, and ensuring safety in these sectors.

The major elements involved in steam circuits are as follows:

- Steam boiler. This is the element that converts clean water into steam thanks to several heating elements (electric resistors, fuel, gas, etc.).
- Steam pipelines. Their mission is the transportation of steam in all production processes.
- Pumps. They are used for pumping condensed water to the boiler.
- Steam traps. In a steam pipeline, they are typically installed every 30 to 50 m depending on factors like pipe size and operating conditions. Additionally, steam traps are placed at critical points such as the following:
    - Low points in the piping: to prevent condensate buildup.
    - Changes in elevation: where condensate can accumulate.
    - Before processing equipment: like heat exchangers or control valves.
    - End of steam pipelines: to purge condensate before it re-enters the system.

Steam traps can be classified into three main types based on their operating principles. Mechanical steam traps use a float that rises with the condensate level, opening the valve to discharge water, and then closing once the condensate is removed. Thermodynamic steam traps operate by leveraging the speed difference between steam and condensate; slower condensate flow keeps the valve open, while the higher speed of steam causes it to close. Thermostatic steam traps respond to temperature changes, opening the valve when cooler condensate is present and closing it when hot steam arrives. Figure 2 shows all the steam production and condensed water evacuation processes.

2.2. Steam Trap Operation

For an efficient and secure steam process, steam traps play a vital role. They remove condensate to prevent water hammer, ensuring the safe operation of steam systems. By eliminating condensate, they allow dry, superheated steam to flow freely, improving heat transfer and reducing energy consumption. Additionally, steam traps protect pipes and equipment from corrosion and operational issues while maintaining a stable steam flow, which is essential for optimizing equipment performance and minimizing process interruptions.

Related to this, water hammer is a dangerous phenomenon caused by the sudden stopping or redirection of steam or condensate flow, generating high-pressure waves that can severely damage pipes, valves, and critical components such as heat exchangers and pumps. This issue is particularly severe in steam systems due to the high pressures and temperatures involved. Beyond physical damage, water hammer poses significant safety risks, as pipe failures can lead to high-pressure steam leaks, endangering workers and facilities. Additionally, it can disrupt continuous steam flow, causing equipment shutdowns, reduced production efficiency, and considerable economic losses. Frequent repairs due to water hammers also result in increased maintenance costs, including labor and replacement parts. Moreover, when a steam trap leaks, the resulting annual energy and cost losses can be substantial, depending on the volume of steam lost, operating pressure, and duration.

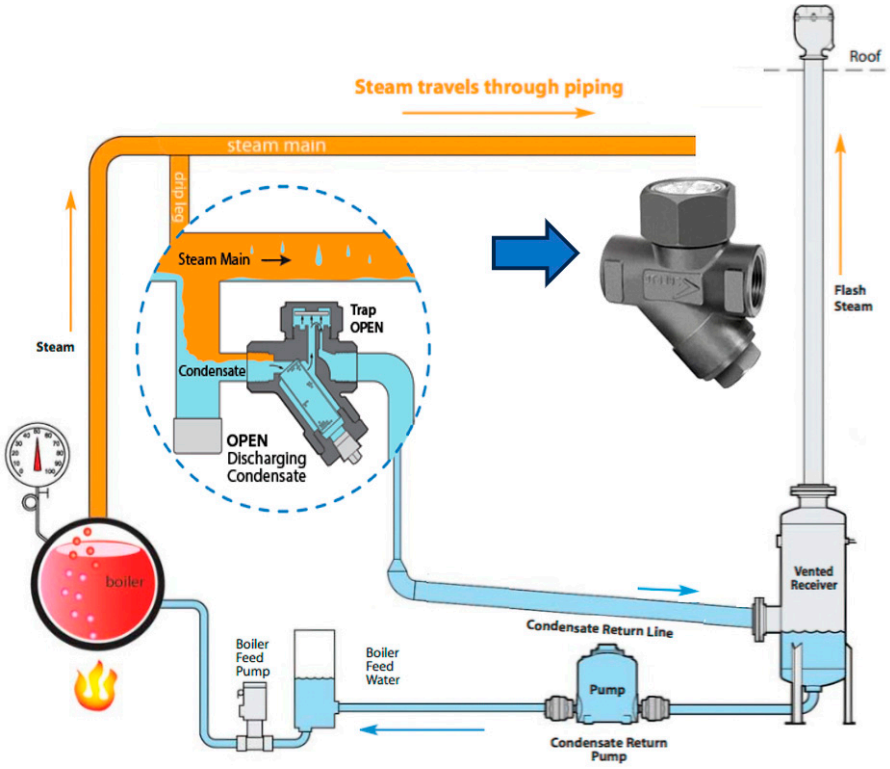

Figure 2. Steam circuit composed of the boiler, steam pipeline, and steam trap.

2.3. Steam Trap Failures

The probability of steam trap failure in a steam circuit is influenced by factors such as trap type, operating conditions, maintenance quality, and the environment [7]. Industry data indicate that annual failure rates range from 5% to 25%, depending on maintenance practices, with well-maintained systems exhibiting failure rates below 10%, while poorly maintained ones can exceed 25%. Common causes of failure include sediment or calcium buildup, internal leaks, insufficient discharge, mechanical wear, corrosion, and extreme operating conditions like incorrect pressure or temperature. Failure rates also vary by trap type: thermodynamic traps are robust but require regular maintenance to avoid failure rates of 10–15%; float traps are more susceptible to sediment accumulation and mechanical issues, with failure rates of 15–20%; and thermostatic traps are prone to debris and temperature control issues, resulting in failure rates of 15–25%.

2.4. Steam Leak Cost Estimation

One of the major energy inefficiencies in manufacturing industries that use steam in their processes is the steam leaks in boilers, pipelines, and mainly steam traps [8].

When a steam trap is leaking, the annual losses can be significant in terms of energy and costs. Depending on the amount of steam lost, the pressure, and the operating duration, the losses can be substantial. Below is an estimation of potential losses:

Estimation of Steam Losses:

A steam trap leaking 0.5 kg of steam per minute can result in the following:

1. Steam Loss:
   - Per hour: 0.5 kg/min × 60 min = 30 kg of steam/hour.
   - Per day: 30 kg/h × 24 h = 720 kg of steam/day.
   - Per year: 720 kg/day × 365 days = 262,800 kg of steam/year.

2. Energy Costs: The cost of producing steam generally ranges between EUR 3 and 10 per ton of steam (1000 kg), depending on fuel type and boiler efficiency. Assuming an average cost of EUR 5 per ton, 262.8 tons × EUR 5/ton = EUR 1314 per year for each leaking steam trap. Therefore, in a mid-sized oil refinery with 10,000 steam traps with a poor maintenance process, assuming an annual failing estimation of 25%, the overall energy loss reaches EUR 3.3 M yearly.

This issue has several additional repercussions [9]. Steam losses are exacerbated in systems with higher pressure or larger steam traps, potentially doubling or tripling the economic impact. In industrial plants with dozens or hundreds of steam traps, these losses can accumulate rapidly, amounting to tens of thousands of euros annually if proper inspection and maintenance are neglected [10]. Furthermore, boilers must compensate for lost steam, increasing fuel consumption and contributing to higher greenhouse gas emissions, such as CO_2. Steam losses also reduce the overall efficiency of the system, negatively impacting industrial processes that depend on specific steam pressures and temperatures [11]. These energy and cost losses are highly influenced by the steam pressure and the orifice size of the steam trap, as demonstrated by Napier's equation in Figure 3.

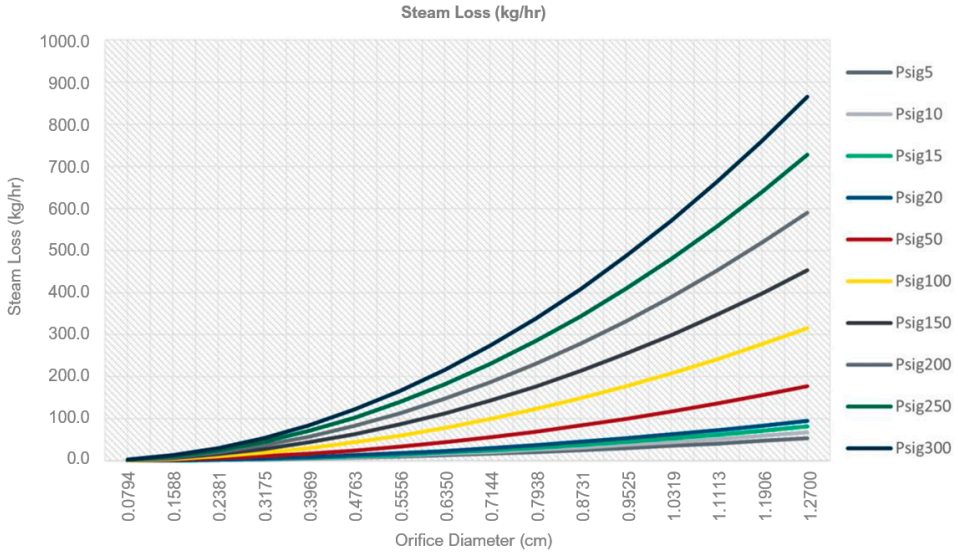

Figure 3. Napier's equation representing steam loss in Kg per hour.

3. Present Technology Scenario

3.1. Detection of Steam Losses in Steam Traps

After evaluating the criticality of steam leaks, it is essential to determine when a steam trap is malfunctioning. Detection methods range from non-intrusive approaches, which do not interfere with the steam process, to intrusive methods that require installing sensors inside the steam trap. Non-intrusive methods include visual inspections, where the continuous venting of live steam, rather than intermittent condensate discharge, signals a malfunction. Temperature profiling using infrared thermography or surface sensors can also help detect leaks by comparing inlet and outlet temperatures; if both are similar, it may indicate steam escape. Additionally, ultrasonic detection devices identify the high-frequency sounds of steam leaks, distinguishing them from the lower frequencies associated with normal condensate discharge. Intrusive methods involve installing flow meters or differential pressure gauges at the discharge line to quantitatively detect abnormalities, such as continuous or excessive flow, which indicate steam leakage.

3.2. Actual Sensing Devices

In order to perform automatic steam leaks detection, there are several commercial technologies offering different sensors and wired/wireless technologies. We summarize the following options:

- **Wireless** using conventional Wi-Fi, Bluetooth, or WirelessHart. These devices detect inlet and outlet temperatures for monitoring. They are powered by lithium batteries with an overall expected lifetime of 2 years. Due to the high battery consumption, data are only sent once per day. We can include an Emerson Rosemount acoustic transmitter (only ultrasound) [12] or Loctite Pulse (only temperature) [13] in this system, both of which are compared in Section 5.4.
- **Wired** using a conventional RS485 data communication bus. This device monitors inlet and outlet temperatures and also pressures. It needs an overall power consumption of 100 mW, and data are sent in real time with a costly four-wired infrastructure as used by Purgasa Bitherm [14].

In contrast, this paper introduces a new approach that combines the benefits of both wireless and wired technologies. The proposed solution is autonomous, powered by the heat of the steam trap or pipeline through thermoelectric devices. It features a plug-and-play installation that is non-intrusive and maintenance-free, eliminating the need for replacing lithium batteries or their equivalents. Data are transmitted every five minutes, limited by the LoRaWAN spread factor. The system integrates three sensors: two measuring inlet and outlet temperatures, along with an ultrasound detector for enhanced performance monitoring.

4. Steam Leak Detection

In this section, we introduce the actual heat-powered [15] device designed for detecting steam leaks (Figure 4). It features a highly efficient thermoelectric generator (TEG) coupled with a DC/DC up-converter and an edge-computing, battery-free device. The system incorporates a LoRaWAN wireless protocol chipset for communication. It also includes temperature detection via ΔT (temperature differential) and ultrasound for comprehensive leak detection. The device connects to cloud computing or SCADA systems through a LoRaWAN gateway for data transmission/analysis.

Figure 4. Proposed scenario from the heat-powered IoT device to the cloud platform.

In detail, Figure 5 shows the stand-alone heat-powered IIOT device composed by:

1. Edge-computing IIoT, using LoRaWAN with three sensor interfaces (Section 4.2).
2. TEG device with a housing and radiator, which converts heat into electricity (Section 4.1).

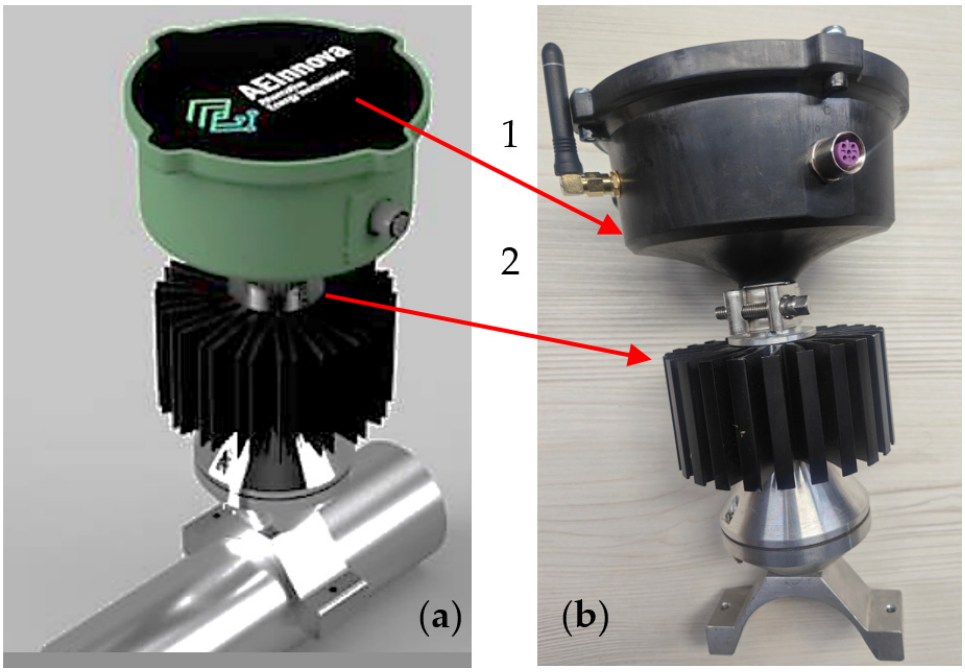

Figure 5. The heat-powered IIoT device is composed of three modules; rendered (**a**) and real (**b**).

4.1. TEG Design

4.1.1. Thermal Model

This device has the mission of generating all the power required for the IIoT and all three sensors.

The overall thermoelectrical converter performance depends on the TEG cell efficiency in the conversion of thermal into electricity. The working principle of the Peltier cell involves the physical effects named Seebeck, Peltier, Thomson, and Joule.

- The Seebeck effect is responsible for the electricity generation in the cell. It takes place whenever two semiconductor materials A and B are joined together at their ends by a conductive material and there is a temperature difference between the two joints. This leads to the conversion of heat into electricity. The Seebeck coefficients account for electromotive force generation (Equation (1)).

$$\frac{\partial E_T}{\partial T} = \alpha_a - \alpha_b \tag{1}$$

where $\frac{\partial E_T}{\partial T}$ is the derivative of the electromotive force with respect to temperature. It represents the voltage gradient generated per unit of temperature change in the system. It is measured in volts per kelvin.

α_a α_b is the Seebeck coefficient (or thermoelectric power) of material a or b, expressed in V/KV. It describes how efficiently material a or b converts a temperature difference into a voltage.

- The Peltier effect is the cooling or heating effect that occurs when an electric current passes through a junction of two materials, as opposed to the Seebeck effect. The heat flux absorbed or rejected by this effect $\dot{Q}_{Peltier}$ is given by Equation (2).

$$\dot{Q}_{Peltier} = \pm IT(\alpha_a - \alpha_b) \tag{2}$$

where I represents the current and T the temperature in the junction.

- The Joule effect accounts for the heating up of a material when current passes through a conductor material. The heat flux $\dot{Q}_{Joule}$ that is produced by this effect is represented by Equation (3), where R_0 is the internal electrical resistance that accounts for this effect.

$$\dot{Q}_{Joule} = R_0 I \tag{3}$$

- The Thomson effect takes place when current passes through a single material that is subject to a temperature gradient along its length. This can lead to both absorption and generation of heat depending on the value of the Thomson coefficients. The heat flux (Equation (4)) is dependent on the Thomson parameter σ.

$$\dot{Q}_{Thomson} = -\sigma I \Delta T \tag{4}$$

The conversion efficiency of a Peltier cell is given as a function of the parameter Z (units 1/K), or the parameter ZT (no units), where T represents the average temperature in the cell. The Z factor relates the energy supplied by the cell to the load with respect to the heat transfer that the cell has. Equations (5) and (6) give the maximum efficiency in terms of the figure of merit ZT used in thermoelectric devices. ZT depends on the temperature T, and the thermoelement parameters α (Seebeck coefficient), σ (electrical conductivity) and k (thermal conductivity). The term $h_c = 1 - T_H/T_C$ is the Carnot Efficiency. In [13], these equations are applied to the model.

$$ZT = \frac{\sigma \alpha^2 T}{\kappa} \tag{5}$$

$$\eta_{max} = \frac{T_H - T_C}{T_H} \frac{\sqrt{1 - Z\overline{\overline{T}}} - 1}{\sqrt{1 + Z\overline{\overline{T}}} - \frac{T_C}{T_H}} \tag{6}$$

Thanks to this model, it is possible to design the most efficient heat harvester and radiator to achieve the maximum ΔT. In detail, the aluminum pipeline (Figure 6a) adapter transfers the heat harvested from the steam pipeline to the TEG hot surface (THot). Thanks to the thermal resistance of the Peltier cell and the radiator coupled to the cold surface (TCold), it is possible to achieve the corresponding ΔT required for energy production. This "heat exchanger" (Figure 6b) extracts all the heat that passes through the Peltier cell and dissipates it through its cooling elements.

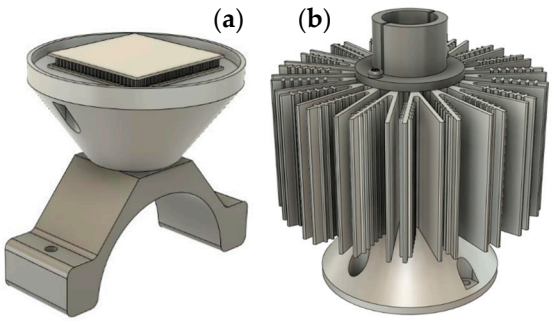

Figure 6. Thermoelectric Peltier housing for the pipeline (**a**) and radiator (**b**) to increase the ΔT.

In Figure 7, a thermal simulation is presented, considering the proposed designs for the thermoelectric module. The simulation accounts for a heat source of 150 °C, a temperature commonly encountered in steam pipelines and steam traps. As demonstrated, the maximum temperature reaching the edge computing device is 65 °C under the worst-case scenario. Additionally, the hot plate (Figure 6a) reaches a temperature of 130 °C, while the cold plate (Figure 6b) stays at 70 °C, resulting in a successful temperature gradient (ΔT) of 50 °C.

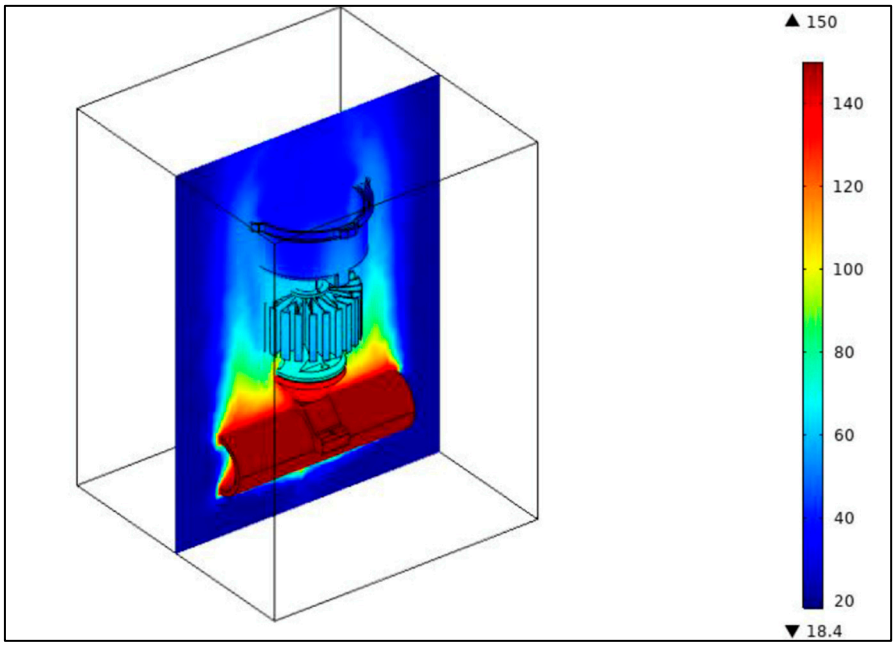

Figure 7. Heat propagation considering 150 °C of heat in the pipeline.

4.1.2. Electronic Design

The power electronic circuit is responsible for converting the energy harvested by each thermoelectric generator module (TGM) into a usable DC output voltage of 3.3 V, which powers the IIoT device. Figure 8 illustrates the power electronics system, which optimizes the operation of the TGMs, ensuring they operate at their maximum efficiency to maximize the harvested thermal energy. Energy is stored in a 5 F supercapacitor able to deliver enough energy to up to five complete acquisition/communication processes.

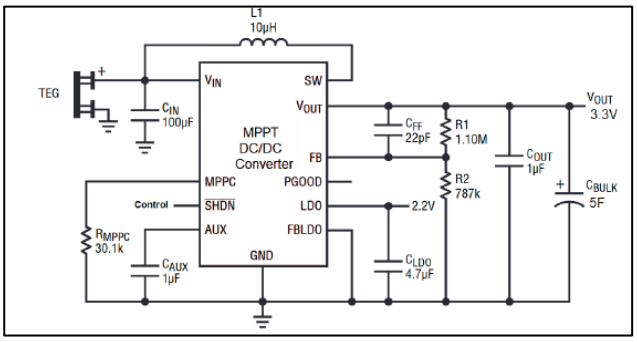

Figure 8. DC/DC up-converter model to stabilize the output voltage at 3.3 V.

Figure 9 shows the main circuit board. In particular, the left image shows the board location inside the PVC case to isolate the electronics from the heat source. In the right image, all subcircuits of the final circuit board are identified.

1. Power management module.
2. LoRaWAN radio interface.
3. Temperature and ultrasound microphone connector.
4. Temperature sensor interface to control the hot surface of the module.
5. Main processor.
6. Programmer interface.
7. Log interface for debugging.

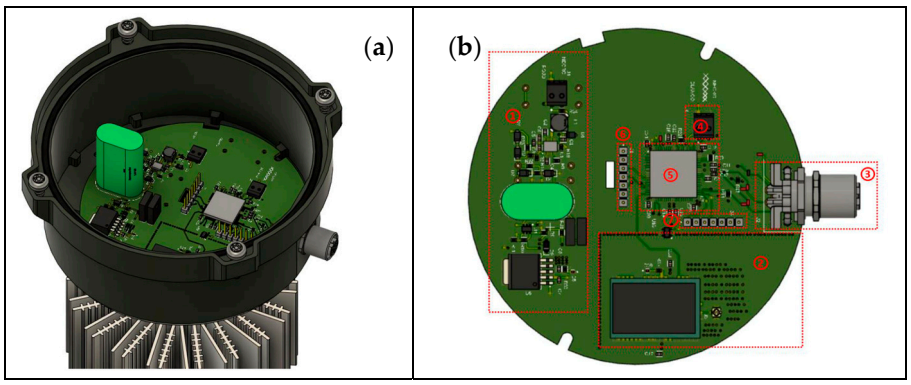

Figure 9. (**a**) Main board location. (**b**) Main board diagram.

4.2. IIoT Module

4.2.1. Wireless Protocol Comparison

In this subsection, we present the technology approach for the wireless IIoT device.

One of the most important things to consider in the wireless sensor networks is the wireless protocol selected. This selection will determine, mainly:

- Node energy consumption.
- Maximum range and the maximum number of nodes connected to the same gateway/repeater.
- Data rate and latency.
- Network costs (licensed or unlicensed bands) and infrastructure costs.
- Node data security encryption.

According to 3GPP and GSMA (Kais et al. [16]), the LoRaWAN protocol is one of the most likely to be adopted in different Low-Power Wide-Area Networks (LPWANs) (Table 1) due to its robustness, range, and ease of scaling.

For our project purposes, the LoRaWAN chipset from the microchip manufacturer RN2483 has been selected [17].

Table 1. LPWAN comparison.

LPWAN Techno	Scada Integration	ATEX/IECEX Compliant	Spectrum	Freq.	Max Data Rate	Range (km)
SigFox	No	Yes.	Unlic.	Regional sub-GHz bands 868/902 MHz	100 bps	3~17
LoRaWAN	Yes	Yes.	Unlic.	Regional sub-GHz bands 433/780/868/915 MHz	50 kbps	2~14
LTE-M.	No	No.	Lic.	LTE In-bands only 1.08/1.4 GHz	1 Mbps	~11
NB-IoT	No	No.	Lic.	LTE In-band, 900 MHz	256 kbps	~22

4.2.2. Hardware Implementation

As previously mentioned, this battery-less LoRaWAN sensing device consists of a DC/DC power converter submodule and a processing submodule (Figure 10 bottom). Additionally, at the top, it shows the main processor subcircuit (Infineon Cypress SoC), responsible for data acquisition, processing, and data formatting, accompanied by the LoRaWAN chipset.

Finally, in Figure 11, the main circuit board including both submodules is shown (power converter and processing/communicating).

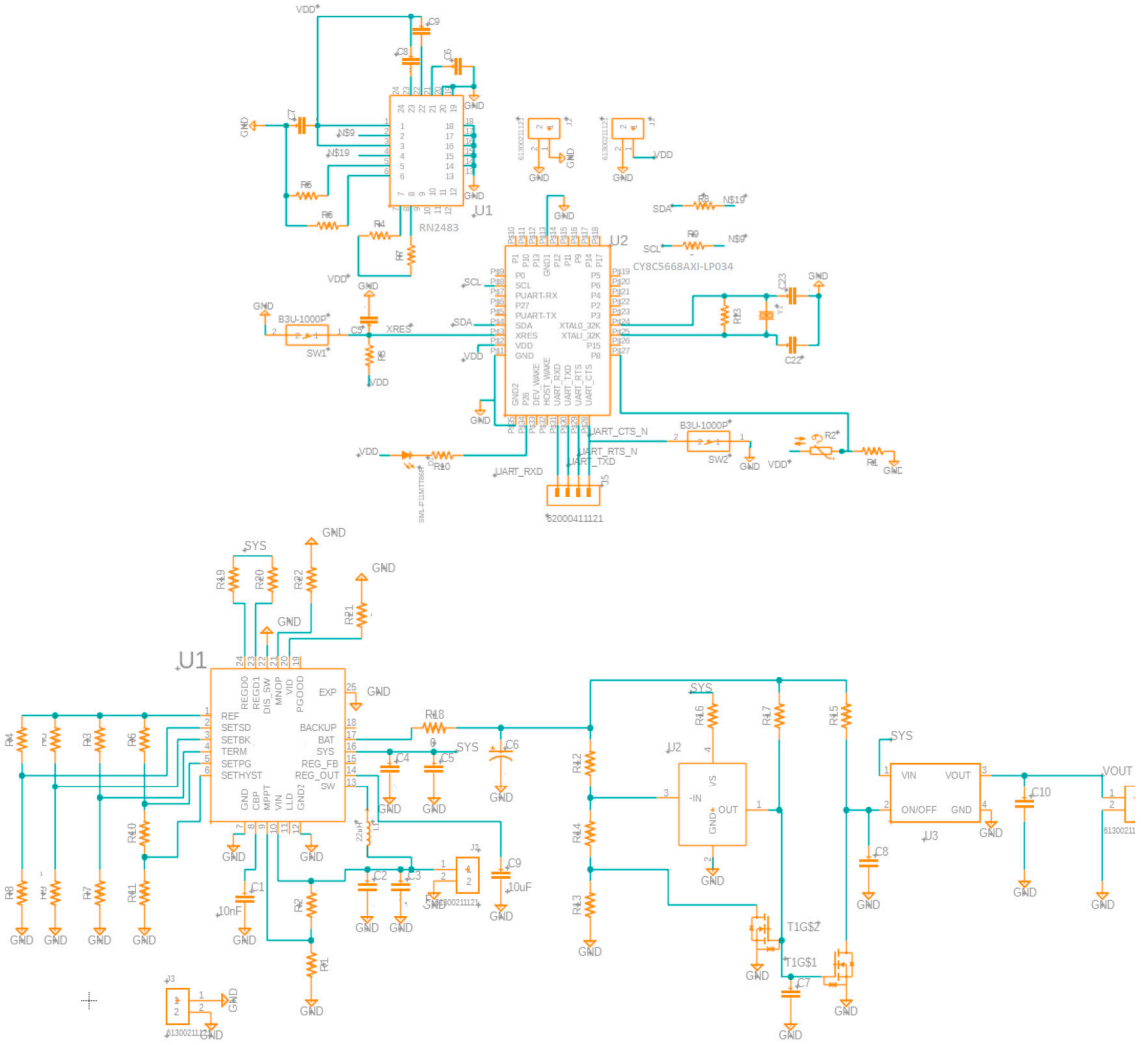

Figure 10. Main board with the data processing and communication subsystem (**top figure**) and the DC/DC conversion and TEG power maximization (**below figure**).

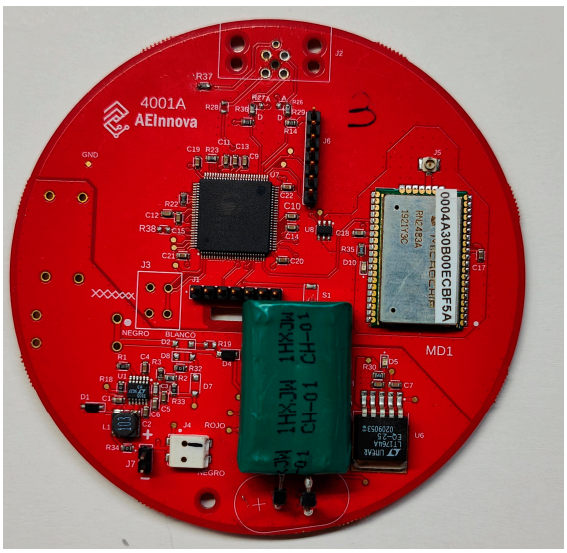

Figure 11. The main board is soldered with all components ready for testing.

4.2.3. Firmware Process

To perform all the processes, we have created the following flow diagram.

Figure 12 shows the complete algorithm that starts by detecting whether there is enough energy stored in the supercapacitor, acquiring both temperatures (inlet and outlet) as well as the sound from the ultrasound microphone. With this information, we will be able to detect if the steam trap is leaking condensed water or steam.

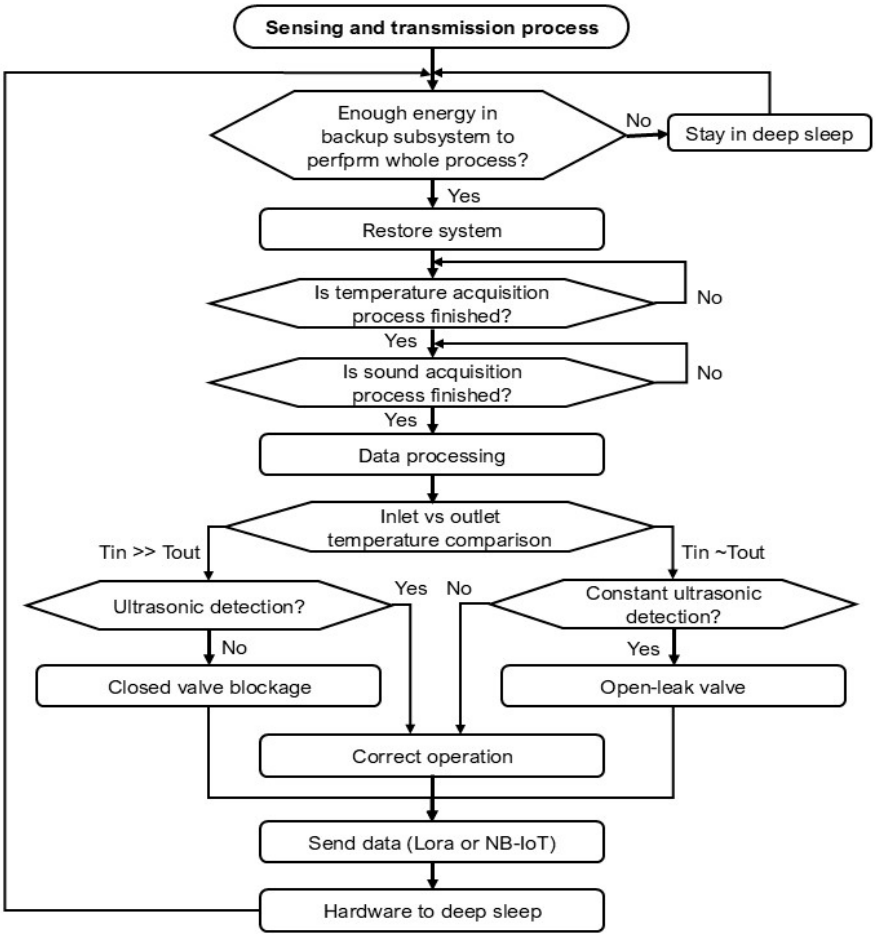

Figure 12. Main algorithm.

5. Main Implementation and Results

This section presents the initial results of the implementation. The first tests were conducted entirely in AEInnova's laboratory, a spin-off of the Microelectronics Department at the Autonomous University of Barcelona, where the authors of this paper are principal founders. Subsequently, the device will be tested under real-world conditions at a pharmaceutical facility located in Barcelona. The Spanish company Hipra, a COVID-19 vaccine manufacturing facility, granted access to perform the first real-world tests on a mechanical (ball float) steam trap.

5.1. Thermoelectric Module Characterization

Initial tests were conducted to characterize the thermoelectric module, located at the lower part of the device. To achieve this, a test bench was developed, consisting of a 2-inch pipeline heated by a 150 W resistor and a support structure for the pipeline (Figure 13, left). The test bench includes a PID controller and a precise PT100 temperature sensor to ensure accurate temperature control of the pipeline surface.

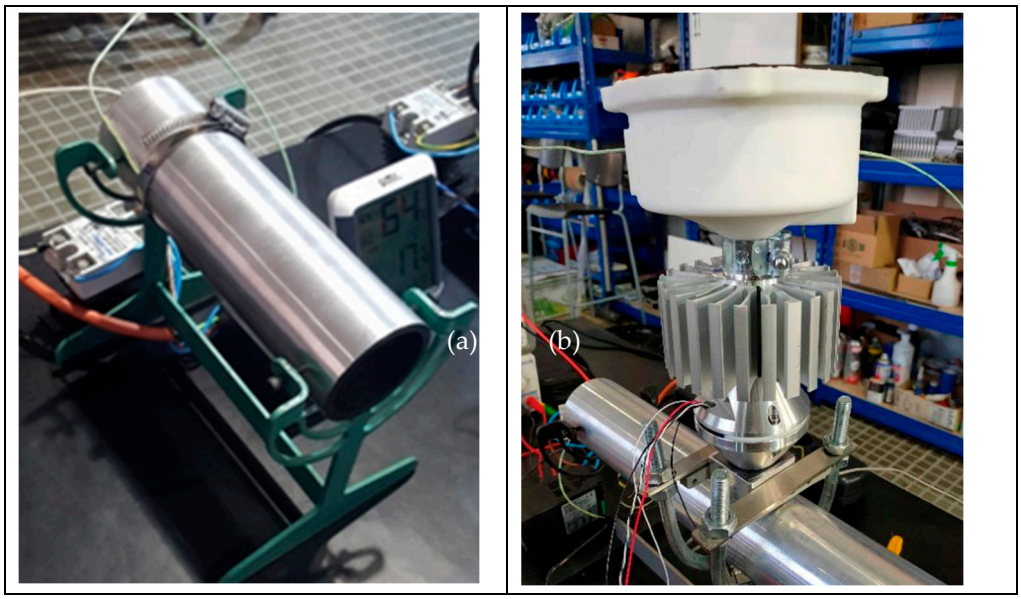

Figure 13. (**a**) The test bench. (**b**) Device under test.

Subsequently, a preliminary version of the all-in-one IIoT system was tested for thermoelectric characterization. The housing for the electronic PCB was fabricated using additive manufacturing (PLA). In the right image of the figure, the device is appropriately positioned on the test bench for measurement. For the measurements, the temperature was increased in increments of 10 °C, with a 20 min stabilization period for the thermoelectric generator (TEG) surface temperature at each step.

The initial test (Figure 14) demonstrates excellent linearity of the open-circuit voltage concerning the temperature of the hot surface on the test bench. The test was conducted over a range of pipeline surface temperatures from 50 °C to 170 °C, across five ambient temperatures (from 15 °C to 40 °C). A maximum voltage of 3.687 V was recorded when the pipeline surface reached 170 °C and the ambient temperature was 15 °C.

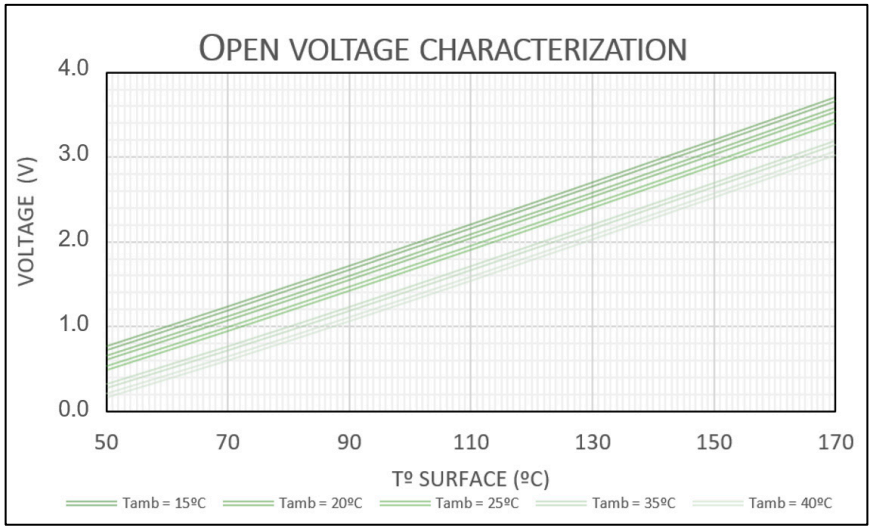

Figure 14. Open-circuit voltage characteristics with a set of hot and cold surface temperatures.

In addition, a series of performance tests were carried out to determine the maximum power output of the device. The thermoelectric generator (TEG) produced a peak power output of 1.034 W under the same conditions (170 °C surface temperature and 15 °C

ambient temperature), which is sufficient to ensure the real-time operation of the IIoT device. The results are shown in Figure 15.

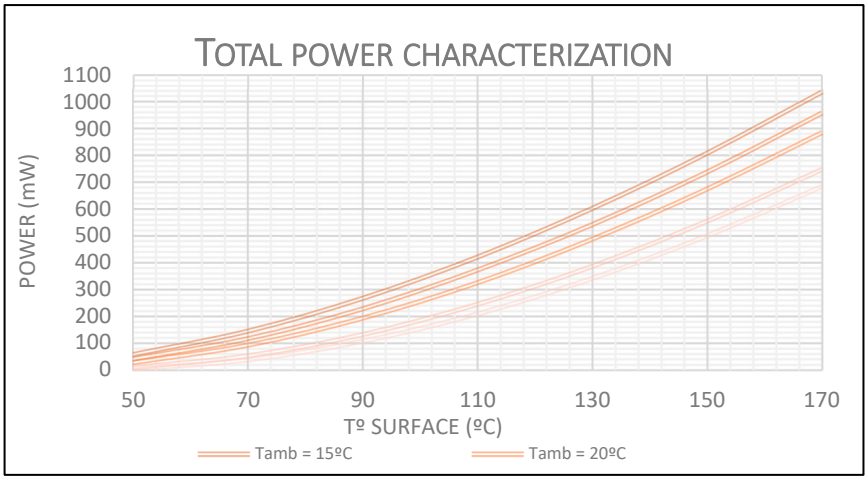

Figure 15. Power generation characteristics with a set of hot and cold surface temperatures.

5.2. Device Characterization in an Uncontrolled Environment

In this section, the device was characterized in an uncontrolled environment (Figure 16). The system was installed on a buoy steam trap, also known as a mechanical steam trap (Figure 16a). To monitor the steam and condensate temperatures, two PT100 temperature probes were placed at the inlet and outlet of the steam trap. Additionally, an ultrasonic microphone with a 50 kHz bandwidth was installed on the steam trap, and data acquisitions were performed at a sampling rate of 100 kbps.

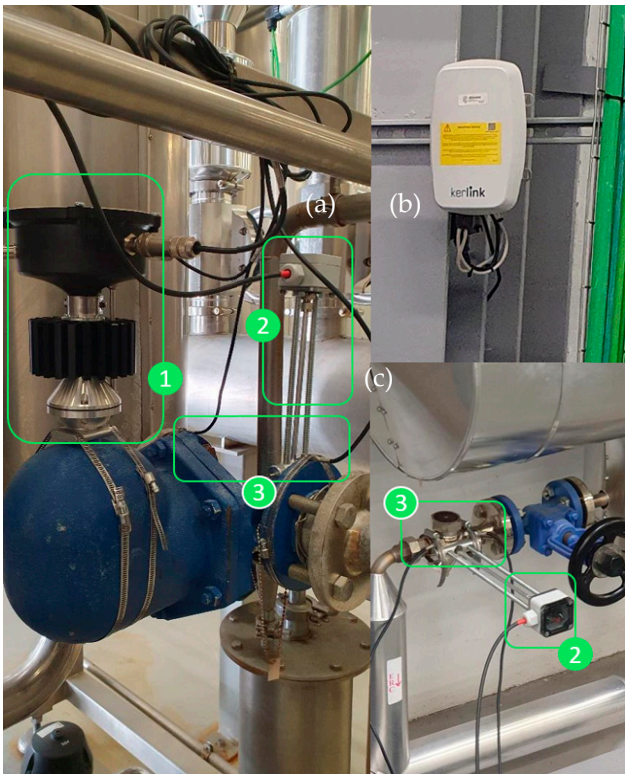

Figure 16. (**a**) Test of buoy steam trap. (**b**) The gateway. (**c**) Test of the thermodynamic steam trap.

To protect the microphone membrane from the heat generated by the steam trap, a capsule was developed to maintain a 30 cm separation between the microphone and the

trap. To transmit the sound between the steam trap and the microphone, an aluminum waveguide was designed, effectively reducing the temperature by nearly half. Also, it is possible to show the LoRaWAN Wirnet Kerling gateway (b).

The same results were obtained in a second set of tests monitoring a thermodynamic steam trap (Figure 16c). In Figure 16, the following are detailed:

1. The heat-powered all-in-one IIoT.
2. The ultrasound microphone.
3. The inlet and outlet PT100.

5.3. Data Analysis

The primary results focus on the discharge process of a steam trap. By utilizing the measured inlet and outlet temperatures (as shown in Figure 17), along with ultrasound measurements, it is possible to differentiate between the normal operational state of the steam trap and potential failures, such as valve leakage (open) or valve blockage (closed). In Figure 17, we have emphasized the region where the steam trap is leaking steam in brown. It is thanks to ultrasound that the leakage was detected. The duration was approximately 40 min per cycle.

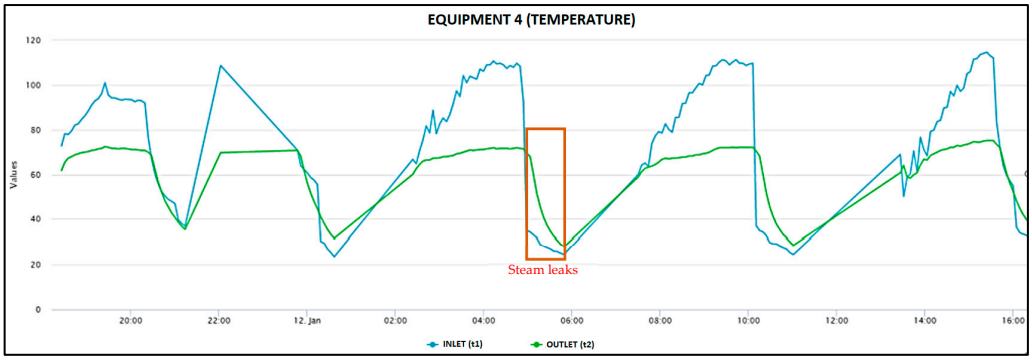

Figure 17. Steam leak detection using delta temperatures between inlet and outlet.

5.3.1. Use of Temperature to Determine the State of the Steam Trap

Normal Operating State:

During normal operation, the steam trap continuously discharges condensate produced within the system, which is mixed with flash steam. As a result, a steady flow of condensate with a small amount of steam passes through the steam trap. This leads to a temperature difference between the inlet and outlet of the steam trap, where the inlet temperature is expected to be higher than the outlet temperature.

Operational Failure: Valve Open (Leakage):

In the event of a leak, the conditions on both sides of the steam trap become equal, resulting in the inlet and outlet temperatures converging. Specifically, the inlet temperature remains constant, while the outlet temperature rises to match the inlet.

Operational Failure: Valve Closed (Blockage):

If the steam trap experiences a blockage that halts condensate discharge, the temperature at the inlet will decrease as the pipe becomes fully flooded with condensate. The outlet temperature will further decrease due to the absence of steam flow.

5.3.2. Use of Ultrasound to Determine the State of the Steam Trap

Relying solely on temperature measurements for analyzing steam trap leakage can lead to errors, as condensate at elevated temperatures may convert to flash steam upon entering a lower-pressure system. In such cases, the temperature of the condensate matches that of the flash steam, making it difficult to distinguish between normal discharge and

leakage based on temperature alone. Ultrasound measurements provide a more reliable method for differentiating between these conditions.

Figure 18 illustrates some of the frequency domain samples, highlighting the signal delta caused by steam passing through the trap around 37 kHz.

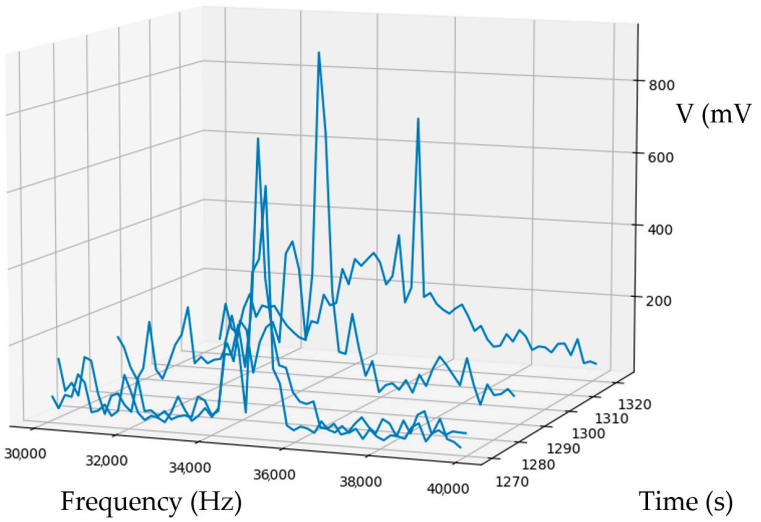

Figure 18. Steam leak frequencies between 30 kHz and 40 kHz.

While many applications monitor sound frequencies around 25 kHz, this range is often contaminated by industrial noise, as shown in Figure 19. To minimize interference, we focus on frequencies between 30 kHz and 40 kHz.

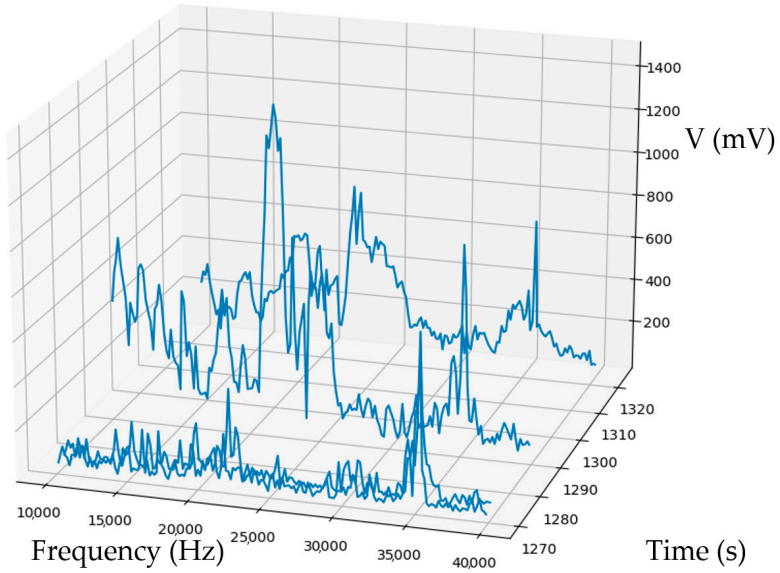

Figure 19. Steam leak frequencies between 10 kHz and 40 kHz.

Our device includes a tuning band-pass filter within the 30 kHz to 40 kHz range.

5.4. Background and Related Work

To provide a comprehensive analysis of the potential market and competitive landscape, Table 2 has been developed to systematically compare existing technologies with our proposed solution. This comparison evaluates our solution combined with five leading manufacturers that offer systems for monitoring steam trap performance. The table outlines key parameters, including technological approaches, functional features, target industries,

and communication protocols. Notably, all competing devices rely either on battery power (integrated with wireless communication protocols) or wired power (e.g., Modbus).

Table 2. Comparison of commercial steam traps.

Manufacturer	Product	Main Tech	Key Features	Target Industry	Comm. Protocol
Spirax Sarco	STAPS	Ultrasound and temperature	- Real-time wireless monitoring. - Compatible with ATEX.	General industry (petrochemical, manufacturing, etc.)	WirelessHART
Gestra [18]	SPECTORcompact	Conductivity	Different conductivity of the pipe with steam.	Industrial processes with high steam demand.	RS485/Modbus
Armstrong International [19]	SteamEye	Ultrasound and temperature	- Non-contact system. - Simple and fast installation.	Manufacturing, power generation, healthcare.	Proprietary RF (radiofrequency)
Henkel (Loctite)	Pulse Smart Steam Trap	Temperature	- Continuous analysis via app.	Chemical, oil and gas, industrial plants.	BLE
AEInnova (this paper)	Leak sense	Ultrasound and temperature	- Real-time. - Non-contact system. - Edge/cloud comp. - Long-range wireless.	General and ATEX industries.	LoRaWAN
Emerson Rosemount	Acoustic transmitter	Ultrasound and temperature	- Real-time. - Non-contact system.	General and ATEX industries.	WirelessHart

Our solution differentiates itself through its innovative power system, which utilizes residual heat as an energy source rather than conventional batteries. This unique approach not only reduces dependency on finite energy sources but also aligns with sustainability goals. Additionally, the integration of long-range wireless communication networks further distinguishes our technology. Unlike traditional short-range wireless systems, such as WirelessHART, or wired solutions that require significant investment in gateways and infrastructure, our approach eliminates these costly requirements. By leveraging energy harvesting and long-range connectivity, our solution offers a more sustainable, cost-efficient, and scalable alternative for industrial monitoring applications, setting a new benchmark in the field.

These solutions demonstrate the diversity in technologies and protocols available to cater to specific industrial needs, from real-time wireless communication (WirelessHART, BLE, RF) to reliable wired options like Modbus.

6. Conclusions

This paper presented a novel Internet of Things (IoT) device tailored for Industry 4.0 applications. The key innovation of this device is its battery-less and heat-powered design, addressing the challenges associated with using lithium batteries in high-temperature and explosive industrial environments. As such, this sensor is a promising candidate for effective process monitoring in these demanding conditions.

We demonstrated the device's advantages over existing technologies, including autonomy, maintenance-free operation, edge computing capabilities, high data transmission rates, and minimal intrusiveness.

In the context of detecting steam leaks in steam traps, a major challenge lies in selecting the appropriate leak detection method. Relying solely on temperature measurements is insufficient in some scenarios, particularly as temperature data may not always be available in on-site operations. Therefore, additional parameters, such as ultrasonic measurements, are essential for improving system accuracy. Ultrasound technology allows for the differentiation between liquid and steam, as steam generates a high-frequency hissing sound, whereas liquid does not. Additionally, it enables easy detection of blocked valves due to

the absence of high-frequency sound signals. Unfortunately, both steam traps monitored during the two-day test period were newly installed, and no issues were detected during the testing window provided by the facility. However, the device successfully demonstrated, consistent with findings in the literature, its ability to monitor both temperature and ultrasound signals for this specific application.

Author Contributions: Conceptualization, R.A., J.O. and C.F.; methodology, R.A., J.O. and C.F.; software, R.A.; validation, R.A.; formal analysis, R.A.; investigation, R.A.; data curation, R.A., J.O. and C.F.; writing—review and editing, R.A., J.O. and C.F.; visualization, R.A.; project administration, R.A.; funding acquisition, R.A. All authors have read and agreed to the published version of the manuscript.

Funding: This research was funded by (1) the Catalan government of Spain: Linea d'ajuts: Nuclis de recerca industrial I desenvolupament experimental, Projectes Economia Circular. Project name: "INDUEYE: Revalorització del calor residual per a l'eliminació debateries de Liti en sensorització. Grant number 466989 (2) This research was funded by The Spanish National Research Agency (AEI) grant number PID2020-116890RB-I00 (AEI/FEDER, EU) under project WISE. (3) This research was funded by the European Commission: H2020 FET Proactive Harvestore Project under grant number 824072; H2020 EIC Pilot Project InduEye 2.0 under grant number 946845.

Data Availability Statement: All data is available in public funding agencies: Nuclis d'economia circular (https://www.accio.gencat.cat/ca/serveis/innovacio/tecnologia-i-rd-per-a-empresa/nuclis-rd-empresarial/ (accessed on 1 November 2024)), Agencia Estatal de investigación (https://www.aei.gob.es/ (accessed on 1 November 2024)), European Commission FET Proactive Project Harvestore (https://harvestore.eu/ (accessed on 1 November 2024)), AEInnova (https://aeinnova.com/proyectos/ (accessed on 1 November 2024)).

Acknowledgments: We thank Alternative Energy Innovations SL technical staff, and HIPRA for facilitating the pharma plant for the steam leak detection test.

Conflicts of Interest: The author Raúl Aragonés is employed by the company Alternative Energy Innovations, S.L.—AEInnova. Carles Ferrer and Joan Oliver declare that the research was conducted in the absence of any commercial or financial relationships that could be construed as a potential conflict of interest.

References

1. Galov, N. How Many IoT Devices Are There in 2020? *Techjury*, 2 June 2022.
2. Pirson, T.; Bol, D. *Assessing the Embodied Carbon Footprint of IoT Edge Devices with a Bottom-Up Life-Cycle Approach*; Elsevier: Amsterdam, The Netherlands, 2021.
3. Notz, D.; Stroeve, J. Observed Arctic sea-ice loss directly follows anthropogenic CO_2 emission. *Sci. J.* **2016**, *354*, 747–750. Available online: http://science.sciencemag.org/content/354/6313/747 (accessed on 18 December 2024).
4. Max Planck Society. How Each One of us Contribute to Arctic Sea Ice Melt. *ScienceDaily.* Available online: http://www.sciencedaily.com/releases/2016/11/161104145708.htm (accessed on 4 November 2016).
5. The Guardian. Available online: https://www.theguardian.com/environment/2016/nov/03/your-carbon-footprint-destroys-30-square-metres-of-arctic-sea-ice-a-year (accessed on 5 January 2024).
6. Aragonés, R.; Alegret, R.N.; Oliver, J.; Ferrer, C. Autonomous Battery-Less Vibration IIoT Powered by Waste Heat for Chemical Plants Using NB-IoT. *IEEE Sens. J.* **2022**, *22*, 15448–15456. [CrossRef]
7. Spirax Sarco: "Steam Traps and Their Failures" Spirax Sarco Technical Resources. Available online: https://www.spiraxsarco.com/global/en-US/products/steam-traps/fault-detection (accessed on 18 December 2024).
8. *ANSI/ASME: Steam Systems Best Practices for Energy Efficiency*; American Society of Mechanical Engineers (ASME): New York, NY, USA, 2021.
9. Armstrong International: "Steam Conservation Guidelines for Condensate Drainage" Armstrong Inter-national Website. Available online: https://www.armstronginternational.com/wp-content/uploads/Broch_SteamConservationGuidelines_P101D_EN_20-20190501.pdf (accessed on 18 December 2024).
10. Einstein, D.; Worrell, E.; Khrushch, M. *Steam Systems in Industry: Energy Use and Energy Efficiency Improvement Potentials*; Lawrence Berkeley National Laboratory: Berkeley, CA, USA, 2001.
11. Yang, W.; Dixon, A. *Energy Efficiency Potentials in Industrial Steam Systems in China*; United Nations Environment Programme (UNEP) Technology Action Programme: Nairobi, Kenya, 2012.
12. Emerson Rosemount Acoustic Transmitter Website. Available online: https://www.emerson.com/en-us/catalog/rosemount-sku-708-wireless-acoustic-transmitter#:~:text=Featuring%20ultrasonic%20acoustic%20event%20detection%20that%20mounts%20externally,%20the (accessed on 9 January 2024).

13. Loctite Pulse Steam Traps Website. Available online: https://www.henkel-adhesives.com/uk/en/industries/industrial-maintenance-repair/mro-loctite-pulse/steam-trap.html#:~:text=LOCTITE%C2%AEPulse%20Smart%20Steam%20Trap%20is%20a%20predictive%20maintenance%20solution%20that (accessed on 9 January 2024).
14. Purgasa Bitherm Website. Available online: https://bitherm.com/purgador-monitorizado (accessed on 8 January 2024).
15. Aragonés, R.; Oliver, J.; Malet, R.; Oliver-Parera, M.; Ferrer, C. Model and Implementation of a Novel Heat-Powered Battery-Less IIoT Architecture for Predictive Industrial Maintenance. *Information* **2024**, *15*, 330. [CrossRef]
16. Mekki, K.; Bajic, E.; Chaxel, F.; Meyer, F. *A Comparative Study of LPWAN Technologies for Large-Scale IoT Deployment*; ICT Express: Stirling, Australia; Elsevier: Amsterdam, The Netherlands, 2019.
17. Microchip Website. Available online: https://www.microchip.com/en-us/product/rn2483 (accessed on 8 February 2024).
18. GESTA Steam Traps Website. Available online: https://www.gestra.com/global/en-GES/products/steam-traps (accessed on 23 November 2024).
19. Armstrong Steam Eye Website. Available online: https://archive.armstronginternational.com/es/steam-system-testing-monitoring-steameye (accessed on 23 November 2024).